Desalination and Water Treatment
www.deswater.com

doi: 10.5004/dwt.2017.20678

77 (2017) 149–155
May

Assessment of energy saving effects in membrane-based seawater desalination

Minseok Kim[a], Jongmin Jeon[a], Hyunwook Ryu[a], Sangho Lee[b], Suhan Kim[a,*]

[a]*Department of Civil Engineering, Pukyong National University, 45 Yongso-ro, Nam-gu, Busan 48513, Korea, Tel. 82-51-629-6065; Fax: 82-51-629-6063; email: suhankim@pknu.ac.kr*
[b]*School of Civil and Environmental Engineering, Kookmin University, 77 Jeongneung-ro, Seongbuk-gu, Seoul 02707, Korea*

Received 6 October 2016; Accepted 16 December 2016

ABSTRACT

In reverse osmosis (RO) process for seawater desalination, the most important issue is the energy consumption. Intensive efforts have been contributed to freshwater production from seawater at low energy so far. This work analyzes the amount of energy consumption for various energy saving methods proposed by literatures using five commercial RO simulation programs (e.g., CSMPRO Ver 5.0, IMS-Design – 2016, ROSA 9.0, LG Chem NanoH_2O, and Toray DS2). The RO energy consumption can be saved by: (1) adopting high flux RO membranes (0.23–0.67 kWh/m^3), (2) increasing feed water temperature (0.01–0.03 kWh/m^3/°C), (3) increasing RO train size (1.17–1.35 kWh/m^3 for sizing up from 1,000 to 10,000 m^3/d), (4) increasing RO membrane area (0.01–0.02 kWh/m^3/% increase), and (5) decreasing feed concentration (0.02 kWh/m^3/% decrease). If fouling occurs, the RO energy consumption increases by 0.05 kWh/m^3/bar. Comparing the positive effect of energy saving methods and the negative effect of fouling, one can set an optimal strategy for energy saving in RO-based seawater desalination according to a specific situation.

Keywords: Seawater desalination; Reverse osmosis; Energy saving; Fouling

1. Introduction

Reverse osmosis (RO) is one of the membrane-based water treatment technologies and the most widely used desalination process [1,2]. The biggest challenge in RO technology is to produce water at low energy consumption [3–6]. Thanks to the intensive researches, the RO energy consumption for seawater desalination became significantly less than before (e.g., several decades ago).

The theoretical minimum energy consumption for seawater desalination at a recovery of 50% is 1.06 kWh/m^3. However, the actual energy consumption should be larger than the theoretical minimum because the finite-sized RO plants are not operated as a reversible thermodynamic process [4]. High pressure pump (HP) takes the most parts (e.g., 84.4%) in total energy consumption of a typical seawater desalination plant [7]. The energy consumption by HP is highly dependent upon the pump efficiency and the water permeability of RO membrane. The pump efficiency becomes higher as pump capacity increases [1,8], and thus larger RO trains consume lower energy than smaller RO trains. As the water permeability of RO membrane increases, the energy consumption of HP decreases, which is the reason why new materials like carbon nanotube was applied to make super flux RO membranes [9].

Decreasing osmotic pressure of seawater by adopting a pretreatment process can be a good solution to save the HP energy consumption. As the pretreatment process, forward osmosis (FO) and gas hydrate (GH) processes were studied recently [10,11]. FO process is a low-energy desalting process using the osmotic pressure as a driving force, and it is applied to seawater desalination, wastewater treatment, food industry, energy production, and microalgae harvesting [12–18]. Seawater and wastewater effluent are used as draw solution and feed solution, respectively. Diluted seawater by FO process flows into the following RO process with less osmotic pressure compared with that of seawater, which results in the less energy consumption in the FO–RO hybrid desalination

* Corresponding author.

process [10,19]. GH is a crystal compound formed by water and a number of guest gas molecules. In a low temperature and a high pressure condition, GHs form in seawater and are separated from concentrated seawater. The separated GHs are dissociated into guest gas and brackish water in a high temperature and a low pressure condition [11,20,21]. The brackish water produced from the GH process becomes RO feed water with lower osmotic pressure.

There could be other approaches to save the RO energy consumptions such as increasing feed water temperature, reducing RO design flux (or increasing RO membrane areas), and adopting energy recovery devices (ERDs) [4,5]. However, it is difficult to figure out which energy saving methods are better from different sources of literatures because the most previous works have determined the RO energy consumption with inconsistent assumptions (e.g., pump efficiency and RO membrane characteristics). In this study, the various RO energy saving approaches discussed earlier were compared altogether quantitatively under the same standards using commercial RO simulation programs from five different membrane manufacturers [22–26]. Pump efficiency was assumed to be a function of capacity (flow rate) and head (pressure) and was calculated using a commercial RO energy calculation program from an ERD manufacturer [27]. In addition, the negative effect of fouling on the RO energy consumption was investigated and compared with the positive effect of the various energy saving methods.

2. Methods

2.1. RO process design

In order to estimate the positive effect of various energy saving methods, RO process should be designed first. The basic design parameters are as follows:

- $C_f = C_{sw} \cong 35{,}000$ ppm (where C_f and C_{sw} are total dissolved solids (TDS) concentrations of RO feed water and seawater, respectively. Seawater TDS and each ion concentrations in seawater are obtained from literature [28]).
- $C_c \cong 70{,}000$ ppm (where C_c is TDS concentration of RO concentrate. In this case, the recovery rate (r) should be 50%).
- $J_{avg} \cong 15$ LMH (where J_{avg} is the average permeate flux).
- $Q_p = 10{,}000$ m^3/d (where Q_p is the water production rate).
- RO feed water temperature: 5°C–30°C.
- One pressure vessel (PV) contains eight RO elements in series.

The commercial RO simulation software from five different manufacturers (e.g., CSMPRO Ver 5.0, IMS-Design – 2016, ROSA 9.0, LG Chem NanoH_2O, and Toray DS2) [22–26] were used to obtain the RO membrane arrangement (i.e., PV array), feed pressure, and product water quality as the output results using the parameters mentioned above as the input values [10,11,16]. The RO membrane models used for these simulations were selected from the five membrane manufactures. Two types of RO models for each manufacture were taken: one is a standard model and the other is a high-flux model as shown in Table 1.

Table 1
The specification of RO models used in the simulations [22–26]

Membrane type	Area (m^2)	Permeate rate (GPD)	Salt rejection (%)	Boron rejection (%)
A-1	41.0	12,000	99.70	89
A-2	37.0	6,000	99.82	93
B-1	40.9	9,900	99.70	–
B-2	37.2	6,500	99.75	92
C-1	41.0	9,900	99.80	92
C-2	37.0	6,500	99.75	93
D-1	40.9	13,200	99.80	–
D-2	37.1	6,500	99.80	–
E-1	41.0	15,070	99.80	89
E-2	37.0	6,000	99.85	93

2.2. RO energy saving scenarios

Several RO energy saving methods discussed earlier were reflected to the corresponding scenarios as follows:

- Scenario 1 – Adopting high flux RO membranes: the high flux models (A-1, B-1, C-1, D-1, and E-1) were tested in this scenario.
- Scenario 2 – Increasing feed temperature: various RO feed water temperature (5°C, 10°C, 15°C, 20°C, 25°C, and 30°C) were tested in this scenario.
- Scenario 3 – Increasing RO train size: various Q_i (100, 1,000, 5,000, 10,000, and 36,000 m^3/d) were tested in this scenario.
- Scenario 4 – Increasing RO membrane area: various J_{avg} (13, 14, 15, 16, and 17 LMH) were tested in this scenario. Lower flux means larger membrane area to produce the same amount of water.
- Scenario 5 – Decreasing feed TDS: various C_f (7,000, 14,000, 21,000, 28,000, and 35,000 ppm) were tested in this scenario. To maintain C_c (70,000 ppm), the recovery rate is changed to 90%, 80%, 70%, 60%, and 50%, respectively.

If not specified, design parameters for each scenario follow the basic parameters in section 2.1, and A-2 model was selected as RO membrane.

A fouling scenario was introduced to compare the negative effects of fouling with the positive effects of the energy saving scenarios. Assuming 10% decrease in water permeability per year and 10% increase in salt passage per year due to fouling, six different membrane ages (0–5 years old) were set up for the simulation. D-1 and D-2 models were used as RO membranes, and other design parameters are the same as the basic parameters in section 2.1.

2.3. RO energy consumption

In this work, RO energy consumption is assumed to be the same as the sum of the energy consumptions of pumps used in the system (e.g., HP, booster pump (BP), inter-stage pump (IP), and low pressure pump (LP)). All the scenarios except Scenario 4 were assumed to adopt an isobaric type ERD. The flow diagram with an isobaric ERD is shown in Fig. 1.

As shown in Fig. 1, the three pumps (e.g., HP, LP, and BP) are used to operate the SWRO process with an isobaric ERD. Thus, the energy consumption per unit production (E_{RO}, kWh/m^3) can be calculated using the following equation:

$$E_{RO}(\text{kWh/m}^3) = \frac{Q_{HP}P_{HP}/\eta_{HP} + Q_{LP}P_{LP}/\eta_{LP} + Q_{BP}P_{BP}/\eta_{BP}}{36Q_p} \quad (1)$$

where η is pump efficiency, which is calculated using energy recovery's power model [27]. The units of flow rate and pressure are m^3/d and bar, respectively, in Eq. (1). It is assumed that mixing in ERD does not occur, which means $Q_{HP} = Q_p$ and $Q_{LP} = Q_c = Q_{BP}$. P_{LP} and the head loss by ERD are assumed to be 2 bar and 0.9, respectively. The head loss by RO membrane is obtained by the RO simulation, and the pressure of BP (P_{BP}) is the sum of the two head losses by ERD and RO membrane.

In Scenario 5 (decreasing feed TDS), a multi-stage RO system as shown in Fig. 2 should be introduced to achieve higher recovery than 50%. In the multi-stage RO system, the energy consumption can be calculated using the following equation:

$$E_{RO}(\text{kWh/m}^3) = \frac{Q_{HP}P_{HP}/\eta_{HP} + Q_{IP1}P_{IP1}/\eta_{IP1} + Q_{IP2}P_{IP2}/\eta_{IP2}}{36Q_p} \quad (2)$$

When the multi-stage RO system is designed, the minimum required concentrate flow rate per PV (the value is dependent upon the manufacture's guideline) should be satisfied.

3. Results and discussion

3.1. Summary of RO simulation conditions and results

Table 2 summarizes the various RO simulation conditions and results at 25°C (feed water temperature). The six columns from the left end are the input parameters while the five columns from the right end are the output results plus warning messages provided by the manufacturer. The simulation conditions and results for all the energy saving scenarios in section 2.2 except Scenario 2 (increasing feed temperature) are listed in Table 2. In addition, the simulations to see the effect of fouling on the energy consumption were carried out by setting membrane ages from 0 to 5 years old. 10% decrease in water permeability per year and 10% increase in salt passage per year were assumed, and D-1 and D-2 models were used as RO membranes as shown in Table 2.

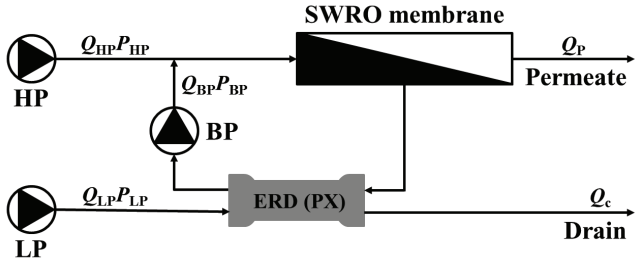

Fig. 1. Seawater reverse osmosis (SWRO) system using an isobaric ERD.

3.2. Energy saving effect

Fig. 3 shows the RO energy consumption with different feed water temperatures and different types of RO membranes (i.e., high flux and standard models). The average values of five RO membranes from five manufacturers were taken to see the overall effect of membrane permeability on the energy consumption (Scenario 1). Selecting high flux RO models can save 0.23–0.67 kWh/m^3, and the energy saving amount increases at lower feed water temperatures. However, one should be very cautious when adopting a high flux RO membrane to design an RO plant because flux or recovery rate of the first RO element placed in the front of PV becomes too high to avoid membrane fouling. As a result, the warning messages about maximum element recovery or flux are shown in the cases of high flux RO models (A-1, C-1, D-1, and E-1) in Table 2. In addition, the product water quality (e.g., TDS and boron concentrations) will become worse when high flux RO models are adopted as shown in Table 2.

Since membrane permeability increases at higher feed water temperatures, the RO energy consumption decreases as temperature increases (Scenario 2). The standard RO models save 0.72 kWh/m^3 when feed temperature increases from 5°C to 30°C while the high flux RO models save 0.29 kWh/m^3 (Fig. 3). Fig. 4 shows the effect of RO train size on the energy consumption (Scenario 3). Because pump efficiency becomes better at larger pump capacities as shown in Fig. 4(b), the RO energy consumption per unit production decreases as RO train size increases (Fig. 4(a)). One important assumption in these calculations is that one HP, one BP, and one LP work for one RO train. The smallest RO plant (100 m^3/d) in Fig. 4(a) shows extremely high energy consumption (e.g., 11.89–14.32 kWh/m^3) because BP with 100 m^3/d does not exist in energy recovery's power model [27], which means the real product does not exist in the market. Thus, ERD is not applied to the RO plant with 100 m^3/d, which is the reason why it shows very high energy consumption in Fig. 4(a).

If more RO elements are added to the RO system with the same water production, the required average flux (J_{avg}) becomes less as shown in Table 2, which results in lower HP pressure and less energy consumption as shown in Fig. 5 (Scenario 4). The amount of energy saving in this scenario is 0.21–0.53 kWh/m^3, which are dependent upon feed water temperature.

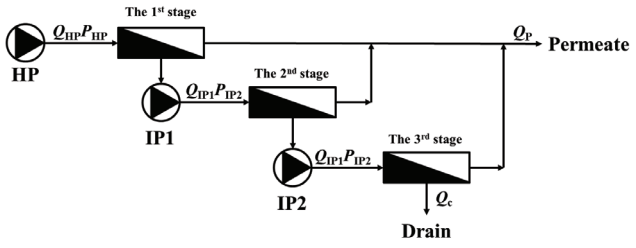

Fig. 2. Multi-stage RO system for high recovery.

Table 2
Summary of RO simulation conditions and results at feed water temperature of 25°C

Input						Output				
Membrane type	Q_p (m^3/d)	r (%)	C_f (ppm)	J_{avg} (LMH)	Membrane age (year)	PV array	P_{HP} (bar)	C_p (ppm)	B (ppm)	Warning message[a]
A-1	10,000	50	35,632	14.82	0	86:0:0	53.8	408	1.71	1, 2
A-2	10,000	50	35,632	14.91	0	94:0:0	60.3	137	0.82	–
A-2	100	50	35,632	14.02	0	1:0:0	59.2	145	0.86	–
A-2	1,000	50	35,632	14.02	0	10:0:0	59.2	145	0.86	–
A-2	5,000	50	35,632	14.91	0	47:0:0	60.3	137	0.82	–
A-2	36,000	50	35,632	14.97	0	337:0:0	60.3	136	0.82	–
A-2	10,000	50	35,632	12.98	0	108:0:0	58.1	157	0.91	–
A-2	10,000	50	35,632	14.02	0	100:0:0	59.2	145	0.86	–
A-2	10,000	50	35,632	15.93	0	88:0:0	61.4	128	0.78	–
A-2	10,000	50	35,632	17.09	0	82:0:0	62.9	120	0.74	–
A-2	10,000	60	28,507	14.91	0	58:36:0[b]	53.3	123	0.72	–
A-2	10,000	70	21,380	14.91	0	48:46:0[c]	45.5	110	0.62	–
A-2	10,000	80	14,253	14.91	0	38:28:28[d]	37.7	97	0.49	–
A-2	10,000	90	7,131	14.91	0	42:32:20[e]	29.6	64	0.31	–
B-1	10,000	50	35,636	14.82	0	86:0:0	57.4	383	2.25	–
B-2	10,000	50	35,636	14.91	0	94:0:0	60.6	218	1.08	–
C-1	10,000	50	35,702	14.82	0	86:0:0	55.1	250	1.28	1, 2
C-2	10,000	50	35,702	14.85	0	94:0:0	59.4	218	0.91	–
D-1	10,000	50	35,632	14.80	0	86:0:0	54.1	360	2.02	2
D-1	10,000	50	35,632	14.80	1	86:0:0	54.6	391	2.22	2
D-1	10,000	50	35,632	14.80	2	86:0:0	55.2	422	2.41	2
D-1	10,000	50	35,632	14.80	3	86:0:0	56.0	452	2.60	2
D-1	10,000	50	35,632	14.80	4	86:0:0	57.0	481	2.77	–
D-1	10,000	50	35,632	14.80	5	86:0:0	58.1	510	2.94	–
D-2	10,000	50	35,632	14.90	0	94:0:0	59.1	147	0.81	–
D-2	10,000	50	35,632	14.90	1	94:0:0	60.7	160	0.88	–
D-2	10,000	50	35,632	14.90	2	94:0:0	62.5	174	0.94	–
D-2	10,000	50	35,632	14.90	3	94:0:0	64.6	187	1.01	–
D-2	10,000	50	35,632	14.90	4	94:0:0	67.0	200	1.08	–
D-2	10,000	50	35,632	14.90	5	94:0:0	69.7	213	1.14	–
E-1	10,000	50	35,663	14.82	0	86:0:0	52.7	363	1.90	1, 2
E-2	10,000	50	35,663	14.92	0	94:0:0	61.0	115	0.81	–

[a]1 – Maximum element recovery has been exceeded. 2 – Maximum element flux has been exceeded.
[b]Q_{IP1} = 8,658 m^3/d, P_{IP1} = 7.7 bar.
[c]Q_{IP1} = 7,183 m^3/d, P_{IP1} = 12.7 bar.
[d]Q_{IP1} = 6,384 m^3/d, Q_{IP2} = 3,187 m^3/d, P_{IP1} = 14.7 bar, P_{IP2} = 4.7 bar.
[e]Q_{IP1} = 4,459 m^3/d, Q_{IP2} = 2,259 m^3/d, P_{IP1} = 1.7 bar, P_{IP2} = 24.7 bar.

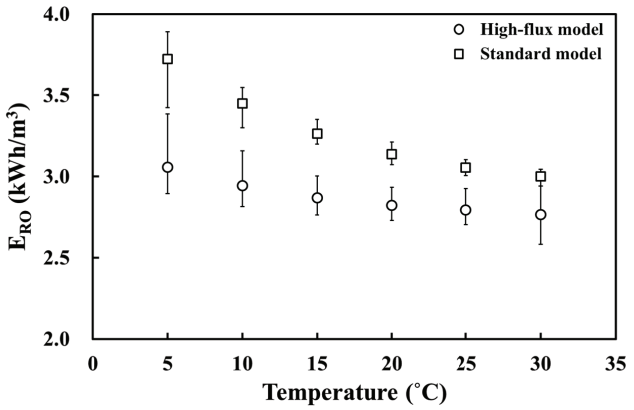

Fig. 3. Effect of membrane permeability and feed water temperature on the RO energy consumption (Scenarios 1 and 2).

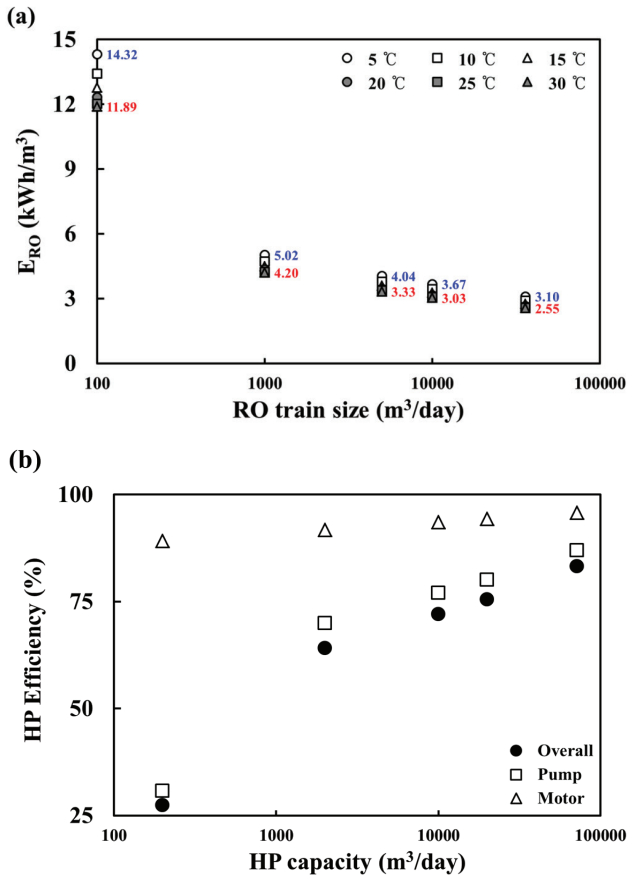

Fig. 4. (a) Effect of RO train size on the energy consumption and (b) effect of HP capacity on the HP efficiency (Scenario 3).

Fig. 6 shows the effect of feed TDS concentration on the RO energy consumption (Scenario 5). The RO energy consumption decreases at lower feed water TDS concentrations because feed osmotic pressure decreases, and thus smaller HP pressure is required. The amount of energy saving is up to 1.73–1.78 kWh/m^3 when feed TDS is decreased to 7,000 ppm. Higher recovery (>50%) can be accomplished with the introduction of multi-stages when feed TDS is

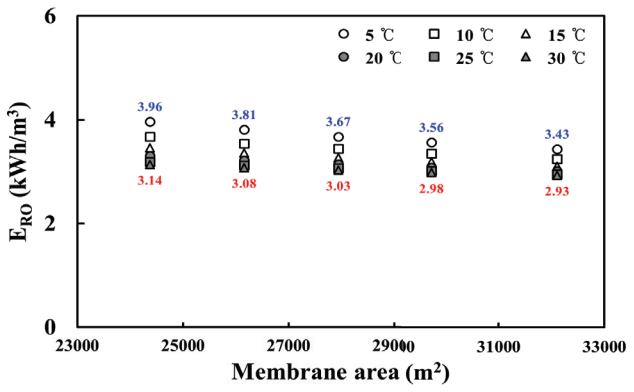

Fig. 5. Effect of membrane area on the RO energy consumption (Scenario 4).

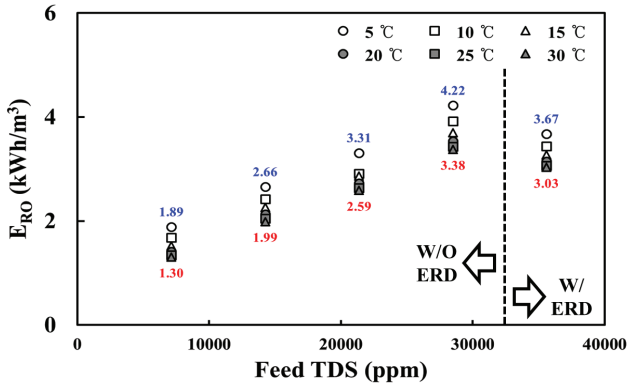

Fig. 6. Effect of feed TDS on the RO energy consumption (Scenario 5).

lower than that of seawater. The higher recovery rates result in the smaller concentrate flow rates, and the introduction of multi-stages results in the larger head loss by RO membranes. For example, RO feed water flows through 16 RO elements (assuming eight elements per one PV) in a two-stage system while it flows through eight RO elements in a single-stage system. Therefore, the energy saving amount of ERD becomes smaller as the recovery increases because the concentrate flow rate and pressure become lower at higher recovery rates. This is the reason why ERD is often ignored in the multi-stage system with higher recovery (>50%) as shown in Fig. 6. When feed TDS is 28,000 ppm, the RO energy consumption is higher than it is when feed TDS is 35,000 ppm because ERD is not adopted (although the energy saving amount of ERD decreases at higher recovery rates). When feed TDS is decreased to >21,000 ppm, the multi-stage RO systems show positive energy saving effect with ERD. Of course, one can adopt ERD to a multi-stage RO system, but it is not suggested due to the increased system complexity (i.e., multi-stages + ERD system) and the less efficiency of ERD at higher recovery rates as discussed above.

3.3. *Effect of fouling*

Figs. 7 and 8 show the effect of fouling on the RO energy consumption and the product water quality (e.g., TDS and

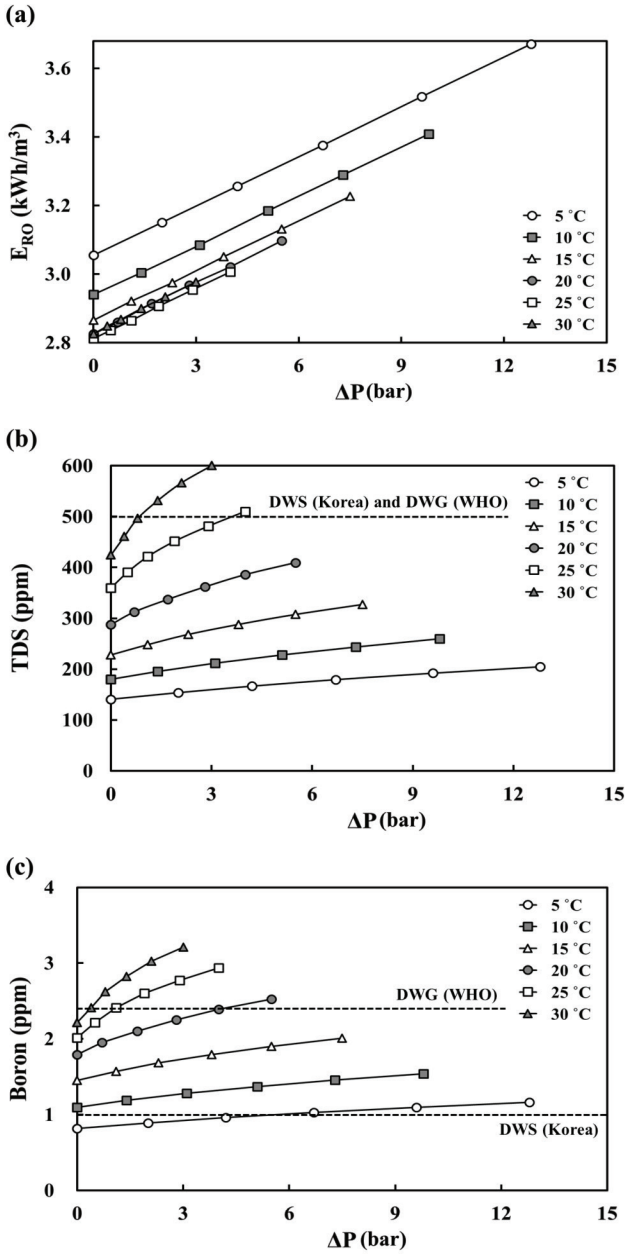

Fig. 7. Effect of fouling on (a) energy consumption, (b) product TDS, and (c) boron concentrations with D-1 membrane (high flux model); DWS (Korea) and DWG (WHO) mean drinking water standard in Korea and drinking water guideline by World Health Organization (WHO), respectively.

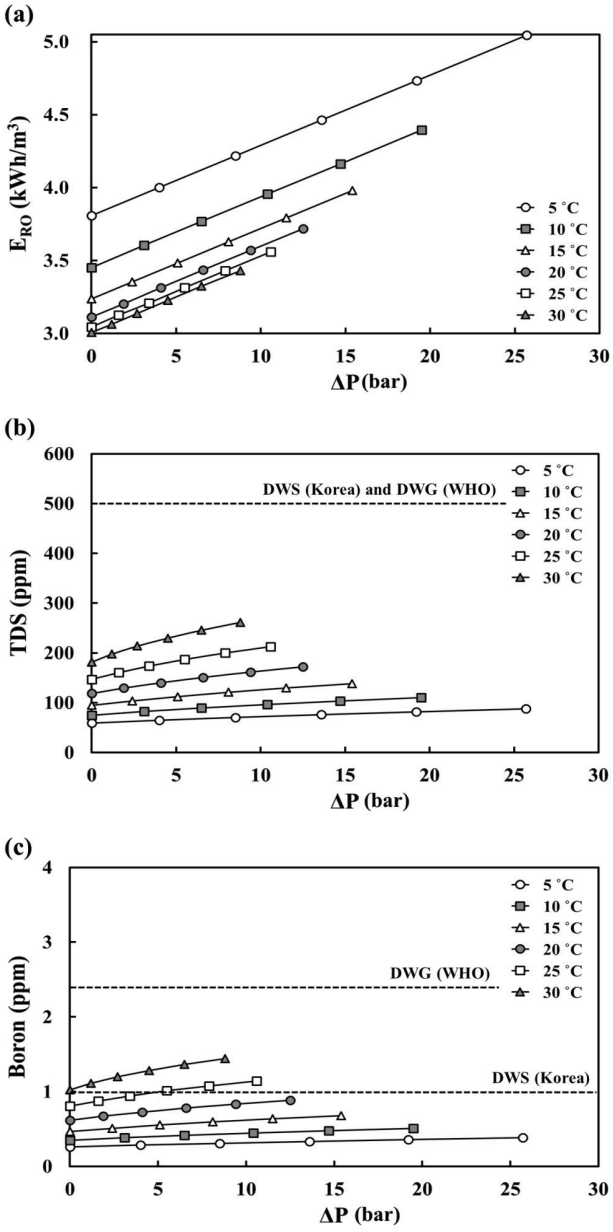

Fig. 8. Effect of fouling on (a) energy consumption, (b) product TDS, and (c) boron concentrations with D-2 membrane (standard model); DWS (Korea) and DWG (WHO) mean drinking water standard in Korea and drinking water guideline by World Health Organization (WHO), respectively.

boron concentrations). ΔP in Figs. 7 and 8 mean the HP pressure difference between the fouled and non-fouled RO membranes. If the same amounts of fouling effects (e.g., 10% of the decreasing rate per year in water permeability and 10% of the increasing rate per year in salt passage) are assumed, the high flux RO membrane (D-1) shows smaller increases in energy consumption (e.g., 0.2–0.6 kWh/m^3) than the standard one (D-2) does (e.g., 0.4 – 1.2 kWh/m^3) as shown in Figs. 7 and 8. However, applying high flux RO membrane has two risks as discussed earlier: (1) the product water quality becomes worse (Figs. 7(b) and 7(c)), and (2) the fouling potential may increase due to high flux and recovery of the lead element in PV as discussed in section 3.2.

4. Conclusions

This work quantitatively analyzed the positive effect of various energy saving methods and the negative effect of fouling on the RO energy consumption using five commercial RO simulation programs. The results are summarized as follows:

- Adopting high flux RO membranes allows 0.23–0.67 kWh/m^3 of energy saving.
- Increasing feed temperature makes 0.01–0.03 kWh/m^3/°C of energy saving.
- Increasing RO train size from 1,000 to 10,000 m^3/d can save 1.17–1.35 kWh/m^3.
- Increasing RO membrane area can save 0.01–0.02 kWh/m^3/% increase.
- Decreasing feed TDS concentration can save about 0.02 kWh/m^3/% decrease (feed TDS concentration should be decreased by 40% at least for energy saving without ERD).
- Fouling wastes about 0.05 kWh/m^3/bar, which means additional 0.05 kWh/m^3 is required as HP pressure increases by 1 bar due to fouling.

Based on the energy saving summary above, we can set an optimal strategy for energy saving in SWRO processes according to a specific situation. For example, if high flux RO models cost 1.3 times more than standard models, increasing membrane areas of a standard RO model by 30% is equivalent to adopting a high flux RO model where the former method saves 0.3–0.6 kWh/m^3, and the latter method saves 0.23–0.67 kWh/m^3. Because a high flux RO membrane is prone to fouling, the former method (i.e., increasing membrane areas) could be an optimal solution to minimize the RO energy consumption. Of course, water product quality should be carefully monitored in each case before the final selection of the energy saving method.

Acknowledgment

This research was supported by a grant (code 16IFIP-B088091-04) from Industrial Facilities & Infrastructure Research Program funded by Ministry of Land, Infrastructure and Transport of Korean government.

References

[1] S. Kim, D. Cho, M.S. Lee, B.S. Oh, J.H. Kim, I.S. Kim, SEAHERO R&D program and key strategies for the scale-up of a seawater reverse osmosis (SWRO) system, Desalination, 238 (2009) 1–9.
[2] S. Kim, B.S. Oh, M.H. Hwang, S. Hong, J.H. Kim, S. Lee, I.S. Kim, An ambitious step to the future desalination technology: SEAHERO R&D program (2007–2012), Appl. Water. Sci., 1 (2011) 11–17.
[3] L. Chekli, S. Phuntsho, J.E. Kim, J. Kim, J.Y. Choi, J.-S. Choi, S. Kim, J.H. Kim, S. Hong, J. Sohn, H.K. Shon, A comprehensive review of hybrid forward osmosis systems: performance, applications and future prospects, J. Membr. Sci., 497 (2016) 430–449.
[4] M. Elimelech, W.A. Phillip, The future of seawater desalination: energy, technology, and the environment, Science, 333 (2011) 712–717.
[5] R. Semiat, Energy issues in desalination processes, Environ. Sci. Technol., 42 (2008) 8193–8201.
[6] J.R. McCutcheon, R.L. McGinnis, M. Elimelech, A novel ammonia-carbon dioxide forward (direct) osmosis desalination process, Desalination, 174 (2005) 1–11.
[7] V.G. Gude, Energy consumption and recovery in reverse osmosis, Desal. Wat. Treat., 36 (2011) 239–260.
[8] N. Voutchkov, Desalination Engineering: Planning and Design, McGraw-Hill, New York, 2012.
[9] C.H. Ahn, Y. Baek, C. Lee, S.O. Kim, S. Kim, S. Lee, S.-H. Kim, S.S. Bae, J. Park, J. Yoon, Carbon nanotube-based membranes: fabrication and application to desalination, J. Ind. Eng. Chem., 18 (2012) 1551–1559.
[10] J. Jeon, B. Park, Y. Yoon, S. Kim, An optimal design of forward osmosis and reverse osmosis hybrid process for seawater desalination, Desal. Wat. Treat., 57 (2016) 26612–26620.
[11] H. Lee, H. Ryu, J.-H. Lim, J.-O. Kim, J.D. Lee, S. Kim, An optimal design approach of gas hydrate and reverse osmosis hybrid system for seawater desalination, Desal. Wat. Treat., 57 (2016) 9009–9017.
[12] F. Lotfi, S. Phuntsho, T. Majeed, K. Kim, D.S. Han, A.A.-Wahab, H.K. Shon, Thin film composite hollow fibre forward osmosis membrane module for the desalination of brackish groundwater for fertigation, Desalination, 364 (2015) 108–118.
[13] S. Zhao, L. Zou, C.Y. Tang, D. Mulcahy, Recent developments in forward osmosis: opportunities and challenges, J. Membr. Sci., 396 (2012) 1–21.
[14] S. Kim, S. Paudel, G.T. Seo, Forward osmosis membrane filtration for microalgae harvesting cultivated in sewage effluent, Environ. Eng. Res., 20 (2015) 99–104.
[15] S. Kim, Scale-up of osmotic membrane bioreactors by modeling salt accumulation and draw solution dilution using hollow-fiber membrane characteristics and operation conditions, Bioresour. Technol., 165 (2014) 88–95.
[16] S.H. Park, B. Park, H.K. Shon, S. Kim, Modeling full scale osmotic membrane bioreactor systems with high sludge retention and low salt concentration factor for wastewater reclamation, Bioresour. Technol., 190 (2015) 508–515.
[17] J. Lee, S. Kim, Predicting power density of pressure retarded osmosis (PRO) membranes using a new characterization method based on a single PRO test, Desalination, 389 (2016) 224–234.
[18] J. Lee, J.Y. Choi, J-S. Choi, K.H. Chu, Y. Yoon, S. Kim, A statistics-based forward osmosis membrane characterization method without pressurized reverse osmosis experiment, Desalination, 403 (2017) 36–45.
[19] T.Y. Cath, J.E. Drewes, C.D. Lundin, A Novel Hybrid Forward Osmosis Process for Drinking Water Augmentation Using Impaired Water and Saline Water Sources, Colorado School of Mines, Golden, CO, 2008.
[20] K.N. Park, S.Y. Hong, J.W. Lee, K.C. Kang, Y.C. Lee, M.G. Ha, J.D. Lee, A new apparatus for seawater desalination by gas hydrate process and removal characteristics of dissolved minerals (Na^+, Mg^{2+}, Ca^{2+}, K^+, B^{3+}), Desalination, 274 (2011) 91–96.
[21] K.C. Kang, P. Linga, K. Park, S.-J. Choi, J.D. Lee, Seawater desalination by gas hydrate process and removal characteristics of dissolved ions (Na^+, K^+, Mg^{2+}, Ca^{2+}, B^{3+}, Cl^-, SO_4^{2-}), Desalination, 353 (2014) 84–90.
[22] Toray Chemical Korea Co. Available at: http://www.csmfilter.com
[23] A Nitto Group Co. Available at: http://membranes.com
[24] The Dow Chemical Co., Available at: http://www.dow.com
[25] LG Chemical, Available at: http://www.lgchem.com
[26] Toray Industries, Inc., Available at: https://www.toraywater.com
[27] Energy Recovery, Inc., Available at: http://www.energyrecovery.com
[28] Dow Liquid Separations, FilmTec Reverse Osmosis Membranes Technical Manual, The Dow Chemical Company Form No. 609-00071-0705, 2005.